High-Affinity CD25-Binding IL-2 Mutants Potently Stimulate Persistent T Cell Growth†

Balaji M. Rao,‡ Ian Driver,‡ Douglas A. Lauffenburger,§ and K. Dane Wittrup*,§

Department of Chemical Engineering and Biological Engineering Division, Massachusetts Institute of Technology, Building 66-552, 77 Massachusetts Avenue, Cambridge, Massachusetts 01239

Received March 8, 2005; Revised Manuscript Received June 3, 2005

ABSTRACT: We have used directed evolution to construct IL-2 mutants that bind the IL-2 α receptor subunit (IL-2Rα, CD25) with affinities comparable to that of the IL-15−IL-15 α receptor subunit (IL-15Rα) interaction. T cells proliferate for up to 6 days following a 30 minute incubation with these IL-2 mutants, which may lead to potential applications for cancer and viral immunotherapy. Several alternative mechanisms have been proposed to explain the contrasting effects of IL-2 and IL-15 on T cell proliferation and death. These IL-2 mutants exhibit T cell growth response−receptor occupancy curves indistinguishable from that for IL-15, suggesting that much of the difference between wild-type IL-2 and IL-15 effects arises simply from their 1000-fold differing affinities for their private α receptor subunits.

IL-2[1] and IL-15 can exert qualitatively differing effects on T cells (*1*−*3*); for example, IL-2 promotes activation-induced cell death (AICD), while IL-15 inhibits AICD. Transgenic mice lacking IL-2Rα exhibit T cell expansion and autoimmune disease (*4*), while IL-15Rα null transgenic mice have reduced numbers of $CD8^+$ T cells and other lymphocytes (*5*). However, paradoxically, both IL-2 and IL-15 signal through the same IL-2Rβ and IL-2Rγ receptor subunits. The mechanisms leading to different biological effects of IL-2 and IL-15 are poorly understood. IL-2 and IL-15 mediate their biological response through a trimeric receptor consisting of shared β and γ subunits and a private α receptor subunit (*6*, *7*). IL-15Rα is expressed in a broad range of cells and tissues, in contrast with IL-2Rα, whose overexpression is in general limited to activated mononuclear cells (*8*). For cells simultaneously expressing the α receptor subunit for both IL-2 and IL-15, there are marked differences in the growth response to IL-2 and IL-15 (*9*). Evidence from fluorescence resonance energy transfer (*10*) and antibodies binding IL-2Rβ at different epitopes (*11*) suggest that the IL-15−IL-2Rβ−IL-2Rγ complex differs topologically from the IL-2−IL-2Rβ−IL-2Rγ complex, and consequently may trigger qualitatively different signals. It has also been proposed that the small cytoplasmic portion of IL-15Rα may be involved in signaling, in contrast with IL-2Rα (*12*). Further evidence for qualitative differences in signaling between IL-2 and IL-15 is that IL-15-mediated proliferation is inhibited to a greater extent than IL-2 by rapamycin inhibition of FKBP (*13*).

We hypothesize that a major contributor to differences between IL-2 and IL-15 is simply altered cell surface receptor occupancy, driven by differing α subunit binding affinities. Both IL-2 and IL-15 bind the IL-2R$\beta\gamma$ heterodimeric receptor with similar affinity ($K_d \sim 1$ nM) and can signal through IL-2/15R$\beta\gamma$ in the absence of the private α receptor subunit. However, they differ starkly in their binding to their private α receptor subunits. IL-15 has a very high binding affinity for IL-15Rα ($K_d \sim 10$ pM), while IL-2 binds with low affinity to IL-2Rα ($K_d \sim 10$ nM) (*7*). This leads to the prolonged persistence of IL-15 but not IL-2 on the surface of T cells, in in vitro assays where cytokine is withdrawn from the medium (*9*). Here we have generated IL-2 mutants with picomolar IL-2Rα binding affinity by directed evolution, and find that the T cell proliferative response to these mutant IL-2 species is essentially the same as responses to equivalent receptor occupancies for IL-15. These results support the hypothesis that IL-2Rβ−IL-2Rγ receptor occupancy is a primary determinant of growth responses for both IL-2 and IL-15.

EXPERIMENTAL PROCEDURES

Generation of IL-2 Mutants. Human IL-2 with a cysteine to serine mutation at position 125 (C125S) was considered wild-type IL-2 (equivalent to Proleukin). A previously described protocol (*14*) was used to express wild-type IL-2 as an Aga2p protein fusion in the EBY100 strain of the yeast *Saccharomyces cerevisiae*. A library of approximately 10^7 yeast-displayed IL-2 mutants (termed "library A") was generated as previously described (*14*).

A soluble, biotinylated form of the ectodomain of human IL-2Rα was a kind gift of T. L. Ciardelli (Dartmouth Medical School, Hanover, NH). An equilibrium binding screen, as previously described (*14*), was used to isolate IL-2 mutants with increased binding affinity for soluble IL-2Rα. WC9 and WE3 are two of the clones with improved IL-2Rα binding

† This work was funded in part by National Institutes of Health Grant CA96504.

* To whom correspondence should be addressed: MIT 66-552, Cambridge, MA 02139. Phone: (617) 253-4578. Fax: (617) 258-5766. E-mail: wittrup@mit.edu.

‡ Department of Chemical Engineering.

§ Biological Engineering Division.

[1] Abbreviations: IL-2, interleukin-2; IL-15, interleukin-15; IL-2Rα, IL-2 α receptor subunit; IL-15Rα, IL-15 α receptor subunit.

10.1021/bi050436x CCC: $30.25
Published on Web 07/14/2005

affinity isolated after two rounds of sorting by flow cytometry.

After one round of sorting of library A, DNA from the pool of mutants isolated was extracted using the Zymoprep kit (Zymo Research Corp.). The mutant IL-2 coding sequences in this pool of DNA were amplified by PCR (termed reaction 1). Concurrently, the mutant IL-2 coding sequences were subjected to random mutagenesis by error-prone PCR in the presence of nucleotide analogues 8-oxodGTP and dPTP to control mutagenesis rates, as previously described (*14*). The product obtained in this mutagenic PCR was amplified further by PCR (termed reaction 2) in the absence of the nucleotide analogues. The products from reactions 1 and 2 were mixed in a 1:1 ratio, and DNA shuffling (*15*) was carried out on the combined pool of DNA. The final PCR product after DNA shuffling was used to generate a library of approximately 1.5×10^8 yeast-displayed IL-2 mutants (termed "library B"), using the protocol described previously (*14*). IL-2 mutants with decreased dissociation rates from soluble IL-2Rα were isolated from library B using a kinetic screen (*16*) with wild-type IL-2 (Chiron) as the soluble competitor. 1a-1, 2-4, and 1b-8 are three of the clones with slower IL-2Rα binding off-rates isolated after four rounds of sorting by flow cytometry.

WC9, WE3, 1a-1, 2-4, 1b-8, and M6, a previously reported IL-2 mutant (*14*, *17*), were chosen in particular for detailed evaluation since they have a range of IL-2Rα binding affinities that bridge the 3 order of magnitude gap in private α receptor subunit binding affinity between wild-type IL-2 and IL-15. Wild-type IL-2 and the IL-2 mutants were expressed solubly in yeast, with an N-terminal FLAG epitope tag and a C-terminal c-myc epitope tag. The mutant IL-2 proteins were secreted in yeast shake-flask cultures. The supernatant was concentrated and purified using a FLAG immunoaffinity column (Sigma). The protein content of each elution was measured on a Cary 50 Bio UV−visible spectrophotometer (Varian). The four elutions containing the highest protein content were pooled. The pooled fractions were then run on a 15% acrylamide gel and stained with Coomassie Blue (0.25 g of Coomassie Blue R-250, 100 mL of ethanol, and 100 mL of water) overnight. To further purify the IL-2 proteins, they were separated by size exclusion chromatography on a Sephadex column on a fast performance liquid chromatography (FPLC) system (Pharmacia Biotech). The eluent was collected in 1 mL fractions. The fractions containing the peak protein, at the correct molecular weight, were pooled. The pooled fractions were loaded on a 15% acrylamide gel, and protein purity was verified. The pooled fractions were then filtered using 0.22 μm centrifuge tube filters (Costar). Protein concentrations were measured using the Micro BCA protein assay (Pierce) according to the manufacturer's protocol.

Tissue Culture. F15R-Kit cells were a kind gift of T. A. Waldmann (National Cancer Institute, National Institutes of Health, Bethesda, MD). The F15R-Kit cell line is an IL-2-dependent human T cell line with stable overexpression of human IL-15Rα and IL-2Rα (*9*, *18*, *19*). These cells also express IL-2Rβ and IL-2Rγ (fewer than 10 000 copies per cell), though at much lower levels than IL-2Rα and IL-15Rα ($\sim 10^5-10^6$ copies per cell). The IL-15Rα expressed in F15R-Kit cells has an extracellular N-terminal FLAG epitope tag. Cells were cultured in a humidified atmosphere with 5% CO_2, in RPMI 1640 supplemented with 0.5 nM IL-2, 10% heat-inactivated fetal bovine serum, 1 mM sodium pyruvate, 200 mM L-glutamine, and 0.8 g/L Geneticin. Prior to any assay, cells were cultured in medium without IL-2 for 1 day.

Quantifying the α Receptor on Cells. Cell surface IL-2Rα was detected using a mouse monoclonal antibody against human IL-2Rα conjugated with R-Phycoerythrin (PE) (Pharmingen). Cell surface IL-15Rα has an N-terminal FLAG epitope tag and was detected by immunofluorescent staining with mouse monoclonal antibody M2 (Sigma) against the FLAG epitope along with a goat anti-mouse antibody conjugated with PE (Molecular Probes/Sigma). Cell surface-bound IL-15 was detected using mouse monoclonal antibody MAB247 (R&D Biosystems) against IL-15 along with a goat anti-mouse antibody conjugated with PE. Quantum Simply Cellular microbeads (Sigma) were used to quantify the total number of IL-2Rα, IL-15Rα, or cell surface-bound IL-15 molecules on F15R-Kit cells, using the manufacturer's protocol. Briefly, the microbeads and the cells were subjected to identical immunofluorescent staining using antibodies to detect IL-2Rα, IL-15Rα, or cell surface-bound IL-15. The median fluorescence values of distinct microbead populations that bind to known, incremental amounts of mouse immunoglobulin were used to generate a standard curve. The median fluorescence value of the cells labeled to detect IL-2Rα, IL-15Rα, or cell surface-bound IL-15 was used with the appropriate standard curve to determine the number of cell surface α receptor or bound IL-15 molecules in antigen binding capacity (ABC) units.

Binding Assays. F15R-Kit cells were labeled (∼100000 cells/mL) with varying concentrations of soluble wild-type IL-2, IL-2 mutants, or IL-15 (R&D Biosystems) for 30 min at 37 °C and pH 7.4. It should be noted that because the cells are metabolically active under these conditions, endocytic trafficking could perturb the estimate of the binding constant K_d; however, this procedure provides a more accurate estimate for cell surface interleukin levels in the proliferation experiments performed at 37 °C than titrations on ice. The cells were subsequently labeled with a polyclonal anti-c-myc chicken antibody (Molecular Probes) followed by a goat anti-chicken antibody conjugated with Alexa dye (Molecular Probes) on ice, to detect cell surface-bound wild-type or mutant IL-2. Alternately, the cells were labeled with mouse monoclonal antibody MAB247 against IL-15 followed by a goat anti-mouse antibody conjugated with PE on ice, to detect cell surface-bound IL-15. The median single-cell fluorescence was determined using an EPICS-XL flow cytometer. Because of the vast overexpression of IL-2Rα and IL-15Rα ($\sim 10^5-10^6$ copies per cell) relative to IL-2Rβ and IL-2Rγ (fewer than 10 000 copies per cell) (*18*, *19*) on F15R-Kit cells, the fluorescence signal from cell surface-bound cytokine can be assumed to be entirely due to binding to the α receptor subunit.

Estimation of K_d. Equilibrium dissociation constants for binding of wild-type and mutant IL-2 and IL-15 to their respective private α receptor subunit were determined using the equation

$$F_{obs} = \frac{cL_0}{K_d + L_0}$$

where F_{obs} is the observed background-corrected median

Table 1: IL-2 Mutants with Increased IL-2Rα Binding Affinity[a]

protein	mutations	K_d (pM)	66% confidence interval
C125S (WT)	−	30030	ND[b]
WC9	S4P, T10A, Q11R, V69A, Q74P, N88D, T133A	1585	950−2700
M6	V69A, Q74P, I128T	1215	740−2000
WE3	N30S, V69A, Q74P, I128T	778	400−1270
1b-8	K8R, Q13R, N26D, N30T, K35R, T37R, V69A, Q74P, I92T	409	230−690
1a-1	N30S, E68D, V69A, N71A, Q74P, S75P, K76R, N90H	254	150−420
2-4	N29S, Y31H, K35R, T37A, K48E, V69A, N71R, Q74P, N88D, I89V	180	110−300
IL-15	−	76	52−110

[a] F15R-Kit cells expressing IL-2Rα and IL-15Rα were labeled with wild-type IL-2, IL-2 mutants, or IL-15 for 30 min at 37 °C and pH 7.4. The amount of cell surface-bound protein was measured using flow cytometry. Data from two different experiments (Supporting Information Figure 1) were used to estimate K_d values as described (Supporting Information). [b] Not determined.

fluorescence, L_0 is the concentration of wild-type or mutant IL-2 or IL-15 used, and c is the proportionality constant.

Data from two separate experiments were used to determine the K_d values for wild-type and mutant IL-2 and IL-15. For each protein, one global K_d value and a proportionality constant c for each experiment were used in a global data fit procedure. The maximum median fluorescence observed at saturating concentrations of wild-type or mutant IL-2, corresponding to saturation of all cell surface IL-2Rα, should be the same. Therefore, the value of c was constrained so that it was the same for wild-type IL-2 and the IL-2 mutants for each experiment. Even though the complete binding isotherm is not captured in the concentration range considered for wild-type IL-2 and some of the IL-2 mutants, the constraint on c allows a K_d value to be estimated for each IL-2 species. Confidence intervals (66%) were determined using the procedure previously described (*20*).

Persistence Assays. A pulse bioassay, as previously described (*17*), was carried out on F15R-Kit cells with a 100 pM pulse concentration of wild-type IL-2, IL-2 mutants, or IL-15. Briefly, cells were exposed to a 30 min pulse of cytokine and then washed with and resuspended in cytokine-free medium. At different time points after cytokine withdrawal, the amount of cell surface-associated ligand was determined using immunofluorescent staining (as described earlier) and flow cytometry.

Bioassays. A pulse bioassay is the simplest approximation for bolus pharmacokinetics. Pulse bioassays, as previously described (*17*), were carried out on F15R-Kit cells with varying pulse concentrations of wild-type IL-2, IL-2 mutants, or IL-15. The viable cell density was determined over a period of 10 days using the Cell-titer Glo (Promega) assay. The numbers of IL-2Rα and IL-15Rα on the cell surface were determined for the cells used in the pulse bioassay.

RESULTS

IL-2 mutants with a range of affinities for IL-2Rα that approach the affinity of IL-15 for IL-15Rα (Table 1 and Supporting Information Figure 1) were generated using yeast surface display and directed evolution (*14*). We compared the bioactivity of high-IL-2Rα affinity IL-2 mutants with that of IL-15 in a T cell line (F15R-Kit) expressing both IL-2Rα and IL-15Rα subunits, in addition to IL-2Rβ and IL-2Rγ. Pulse bioassays, where cells are incubated in cytokine for only a short period of time, were used to mimic the transient cytokine exposure history typical of bolus pharmacokinetics (*17*). Our objective was to quantitatively analyze the relationships between receptor occupancy and proliferation response for IL-2, IL-15, and a series of IL-2 mutants bridging the 3 order of magnitude gap between them in α receptor subunit binding affinity.

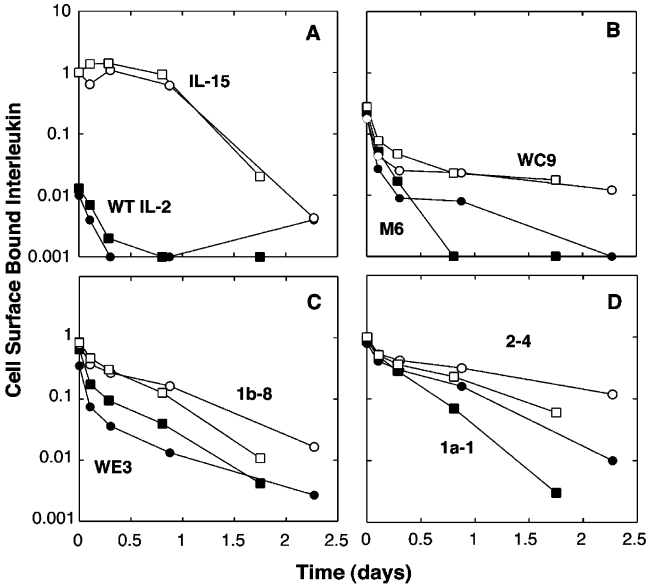

FIGURE 1: Cell surface persistence of wild-type IL-2, IL-2 mutants, and IL-15. F15R-Kit cells (∼100000 cells/mL) expressing IL-2Rα and IL-15Rα were labeled with 100 pM wild-type IL-2, IL-2 mutants, or IL-15 for 30 min at 37 °C and pH 7.4. Cells were then washed with and resuspended in cytokine-free medium. The amount of cell surface-bound protein was measured using flow cytometry at different time points following cytokine withdrawal. The initial (time zero) value corresponds to the cell surface-bound ligand before the wash step. The median fluorescence value for 2-4 at time zero was used to normalize the data for wild-type IL-2 and IL-2 mutants for each data set. The median fluorescence value for IL-15 at time zero was used to normalize data for IL-15, for the data set denoted with empty circles. For the IL-15 data set denoted with empty squares, the K_d value for IL-15 (Table 1) and the experimentally determined total number of IL-15Rα molecules were used to estimate the number of IL-15-bound IL-15Rα molecules at time zero. The number of IL-15-bound IL-15Rα molecules on the cell surface was directly determined for subsequent time points. The number of IL-15-bound IL-15Rα molecules at time zero was used to normalize this data set. Normalized values less than 0.001 are plotted as 0.001.

Increased Cell Surface Persistence of High-IL-2Rα Affinity IL-2 Mutants. In pulse assays, IL-15 persists on the cell surface for more than 2 days, while wild-type IL-2 has negligible persistence on the cell surface (Figure 1A), consistent with previous results (*9*). IL-2 mutants with increased IL-2Rα affinity, however, have greatly increased persistence on the cell surface relative to wild-type IL-2 (Figure 1B−D), since IL-2Rα acts as a ligand reservoir for

high-IL-2Rα affinity IL-2 mutants. Artifactual binding of these IL-2 mutants to IL-15Rα was excluded by the observation that excess IL-15 does not diminish the level of surface labeling by these mutants (Supporting Information Figures 7 and 8). Increased initial private α receptor occupancy after cytokine withdrawal leads to increased cell surface persistence of cytokine over the course of several days (Supporting Information Figure 2). The increased persistence of high-IL-2Rα affinity IL-2 mutants is likely a result of both slower dissociation of the mutants from cell surface IL-2Rα and more efficient recycling of the mutants to the cell surface following internalization, since high-IL-2Rα affinity IL-2 mutants also have improved binding at endosomal pH (data not shown) and conceivably recycle to a greater extent than wild-type IL-2 (*21*). For a given initial receptor occupancy, IL-15 exhibits somewhat greater persistence than the IL-2 mutants (Figure 1 and Supporting Information Figure 2). This may be due to a significantly lower sensitivity of the IL-15−IL-15Rα binding interaction to lowered pH relative to that of the binding of IL-2 mutants to IL-2Rα, and consequently more efficient endocytic recycling to the surface following internalization (Supporting Information Figure 3).

T Cell Growth Response Mediated by High-IL-2Rα Affinity IL-2 Mutants and IL-15. We compared the T cell growth response mediated by IL-15 and high-IL-2Rα affinity IL-2 mutants in a pulse assay to explore the relationship between cell surface persistence and bioactivity. Consistent with previous observations (*9*), IL-15 promotes the growth of T cells in a pulse assay, unlike wild-type IL-2 (Figure 2). An insignificant level of wild-type IL-2 is associated with IL-2Rα on the cell surface following pulse exposure, whereas IL-15 persists in IL-15Rα ligand reservoirs on the cell surface for a prolonged period of time (Figure 1A). Mutants with increasing IL-2Rα binding affinity exhibit prolonged cell surface persistence (Figure 1B−D) and also stimulate improved growth of T cells (Figure 2). Picomolar concentrations of several IL-2 mutants stimulate T cell growth for up to 6 days following a 30 min pulse exposure, while even nanomolar pulse concentrations of wild-type IL-2 fail to produce any net proliferation.

High-IL-2Rα Affinity IL-2 Mutants and IL-15 Mediate Quantitatively Equivalent T Cell Growth Responses. The relationship between T cell growth response and initial receptor occupancy after cytokine withdrawal was quantitatively examined (Figure 3A,B). The maximum viable cell density attained and the integral of viable cell number over a period of 10 days were used as metrics to quantify the family of growth response curves shown in Figure 2. The integral of cell viability as well as the maximum number of cells correlates linearly with the number of interleukin molecules initially captured in cell surface receptor reservoirs (Figure 3A,B), demonstrating the existence of a single pharmacodynamic dose−response curve relating growth to initial receptor occupancy for IL-2, IL-15, and all of the six IL-2 mutants.

IL-2-induced T cell growth is consistent with a quantal signal transduction hypothesis (*22*), by which once the signal mediated through IL-2Rα$\beta\gamma$ exceeds a certain threshold, growth occurs at a specific growth rate independent of the magnitude of the growth signal. The concept of threshold signaling complex levels governing cell fate decisions has additionally found applicability in stem cell biology more broadly (*23*). For an IL-2 (or IL-15)-dependent T cell line such as F15R-Kit, a similar threshold response also converts an actively growing T cell culture to a death phase once the IL-2Rα$\beta\gamma$ signal is depleted below a certain level. To compare the responses to different mutants and different pulse concentrations on a common basis, each growth curve was normalized by its maximum viable cell density (Supporting Information Figure 4) and then aligned on the time axis such that the peak cell number occurs at an approximately common time (Supporting Information Figure 5). All of the IL-2 wild-type and mutant growth curves from Figure 2 map by this procedure onto a single universal growth curve, indicating that the specific growth and death rates are indeed approximately constant (Figure 3C). Consequently, the amount of time spent in the growth phase is sufficient to completely characterize the growth curves in Figure 2. In other words, the growth curves in Figure 2 can be reconstructed from the universal growth curve (Figure 3C) once the initial time (time of cytokine withdrawal) is

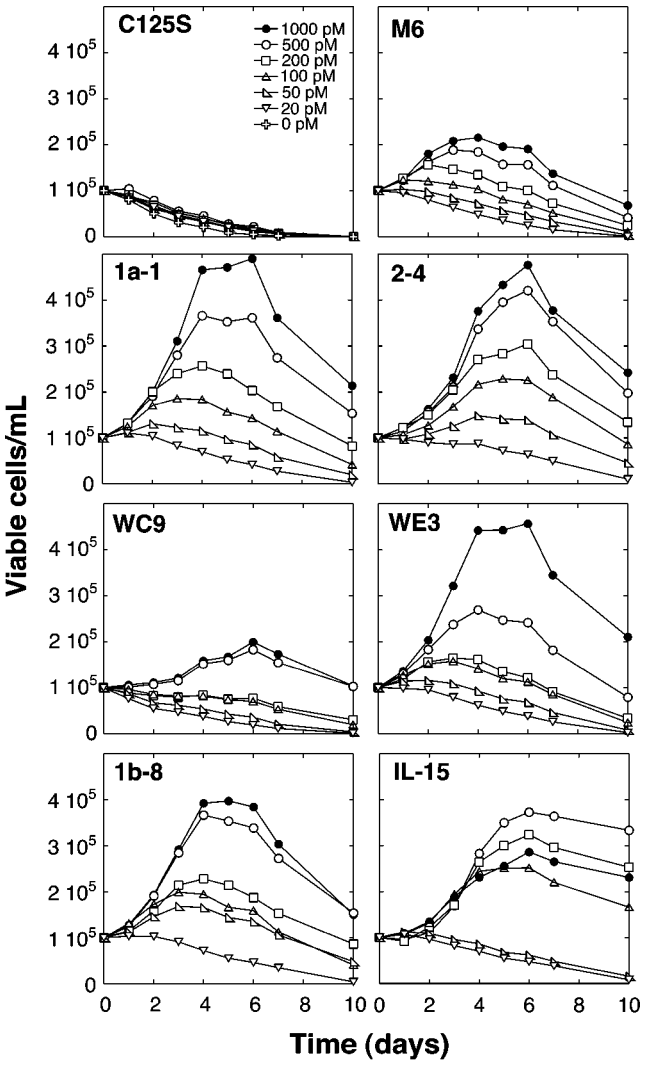

FIGURE 2: IL-2 mutants and IL-15, but not wild-type IL-2, stimulate T cell growth. F15R-Kit cells (∼100000 cells/mL) expressing IL-2Rα and IL-15Rα were incubated with a range of concentrations of wild-type IL-2, IL-2 mutants, or IL-15 for 30 min at 37 °C and pH 7.4. Cells were then washed with and resuspended in cytokine-free medium. The number of viable cells over a period of 10 days was determined using the Cell Titer-Glo (Promega) luminescence assay.

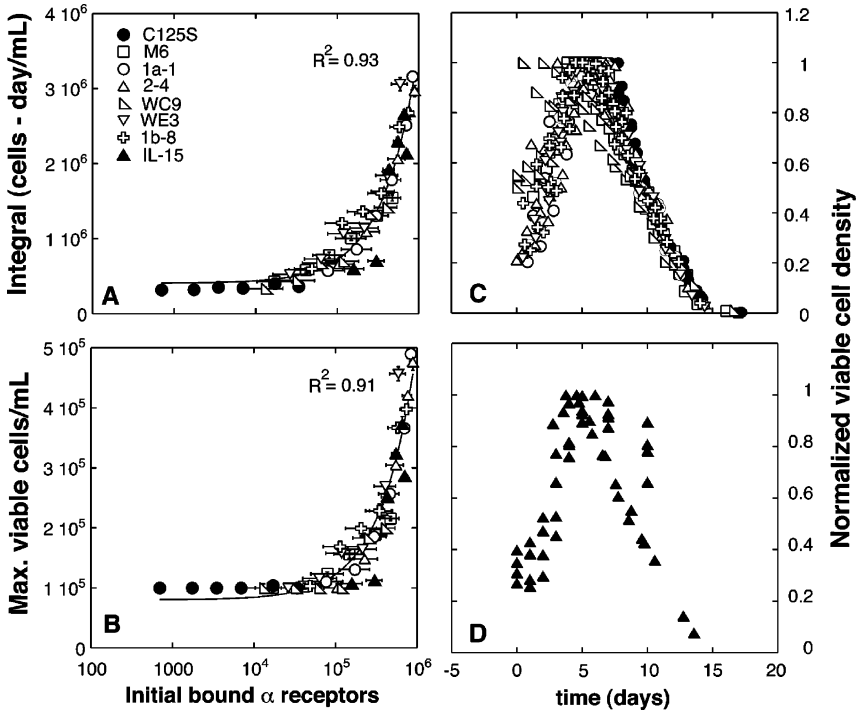

FIGURE 3: Pharmacodynamic response of IL-2 mutants and IL-15 is equivalent (A and B). Growth response of 15R-Kit cells as quantified by the integral of viable cell density over a period of 10 days and the maximum cell density linearly correlate with the initial receptor occupancy for wild-type IL-2, IL-2 mutants, and IL-15. Although the logarithm of surface interleukin is plotted to condense the three-log dynamic range, the relationship is represented well by linear regression with the correlation coefficient R^2. The total numbers of IL-2Rα and IL-15Rα molecules were determined experimentally. The initial receptor occupancy was estimated using K_d values and the total number of receptors. *X*-axis error bars represent the error in estimating the initial receptor occupancy due to error in K_d value estimates. *Y*-axiis error bars represent the standard deviation of triplicate measurements. (C) The growth kinetics of wild-type IL-2 and all IL-2 mutants, for all concentrations, is described by one universal growth curve, indicating that the specific growth and death rates are constant for each culture represented in Figure 2. The normalization and time shift calculations used to convert the growth curves in Figure 2 to this universal curve are detailed in Supporting Information Figures 4−6. (D) IL-15 follows a universal growth curve essentially similar to that of IL-2.

mapped onto the universal growth curve by aligning the time for transition from the growth phase to the death phase, presumed to occur upon depletion of the IL-2Rα$\beta\gamma$ signal below a threshold signal value. The magnitude of the shift on the time axis required to align the curves (time shift) correlates strongly with initial receptor occupancy, with growth maintained for up to 6 days at the highest occupancies achieved with the IL-2 mutants (Supporting Information Figure 6). The growth kinetics of IL-15 are also described by a universal growth curve (Figure 3D), although with somewhat slower death rates than the IL-2 mutants, possibly due to prolonged signaling due to increased persistence of IL-15 relative to any of the IL-2 mutants (panel A vs panels B−D of Figure 1). The very similar universal growth curves for IL-2 and IL-15 (Figure 3C,D) further reinforce the functional equivalence of the pharmacodynamic proliferative response mediated by IL-15 and the high-IL-2Rα affinity IL-2 mutants at equivalent receptor occupancies.

DISCUSSION

We establish here a quantitative relationship between receptor α subunit binding affinity and mitogenic activity for IL-2 and IL-15. Cell surface IL-15Rα, with a high affinity for IL-15, acts as a capture reagent for IL-15 that retains IL-15 on the cell surface for a prolonged period of time and mediates growth of T cells expressing IL-15Rα (*9*). IL-2Rα acts as a similar cell surface ligand reservoir for IL-2 mutants with increased affinity for IL-2Rα. Our results strongly suggest that a primary difference in biological activity between wild-type IL-2 and IL-15 results from their different affinities for their respective private α receptor subunit.

Lymphocyte homeostasis is maintained in vivo by a balance between signals from lymphotrophic survival factors and apoptotic death pathways (*24*). Numerous cytokines with central roles in controlling the number of cells in the lymphoid compartment signal through the common gamma (γ_c) subunit of the IL-2R, IL-2, IL-4, IL-7, IL-9, IL-15, and IL-21, indicating a broad and central role for the growth and anti-apoptotic signal provided by IL-2Rγ_c. It has been hypothesized that differences in the effects of IL-4 and IL-7 relative to those of IL-2 and IL-15 are a result of altered receptor expression on different cell types, rather than qualitatively distinct intracellular signaling pathways (*25*), and our results are consistent with this view. The general approach of creating a cell-bound ligand reservoir might enable engineering of mutant cytokines with enhanced potency for GM-CSF, IL-3, and IL-5 (*26*), since they also possess nonsignaling α capture receptor subunits.

The IL-15-like behavior of high-IL-2Rα affinity IL-2 mutants has potentially significant implications for IL-2-based cancer immunotherapy. IL-2 is FDA-approved for the treatment of metastatic renal cell carcinoma and melanoma (*27*, *28*). At nanomolar concentrations, wild-type IL-2 mediates deleterious toxic effects, through IL-2R$\beta\gamma$ on CD56 dim NK cells (*1*). The increased potency of high-IL-2Rα affinity IL-2 mutants relative to wild-type IL-2 should allow the use of smaller doses, with consequently lower toxicity. The use of IL-15 to replace IL-2 in cancer immunotherapy

has been suggested due to the inhibitory effects of IL-15 on AICD (*3*); however, the broad tissue distribution of IL-15Rα might conceivably lead to detrimental side effects (*7*). IL-2Rα is expressed by activated T cells, so high-IL-2Rα affinity IL-2 mutants should mediate a biological response selectively in these desired target cells. Thus, the IL-2 mutants described here may combine the specificity of wild-type IL-2 with the desired immunotherapeutic effects of IL-15.

ACKNOWLEDGMENT

Soluble IL-2Rα was a kind gift of T. Ciardelli. F15R-Kit cells were a kind gift of S. Dubois and T. Waldmann. Jason Haugh and Jennifer Cochran provided helpful comments on the manuscript.

SUPPORTING INFORMATION AVAILABLE

Binding properties, cell surface persistence, and growth responses to the mutant IL-2 proteins. This material is available free of charge via the Internet at http://pubs.acs.org.

REFERENCES

1. Fehniger, T. A., Cooper, M. A., and Caligiuri, M. A. (2002) Interleukin-2 and interleukin-15: Immunotherapy for cancer, *Cytokine Growth Factor Rev. 13* (2), 169−183.
2. Waldmann, T. (2002) The contrasting roles of IL-2 and IL-15 in the life and death of lymphocytes: Implications for the immunotherapy of rheumatological diseases, *Arthritis Res. 4* (Suppl. 3), S161−S167.
3. Waldmann, T. A., Dubois, S., and Tagaya, Y., (2001) Contrasting roles of IL-2 and IL-15 in the life and death of lymphocytes: Implications for immunotherapy, *Immunity 14* (2), 105−110.
4. Willerford, D. M., et al. (1995) Interleukin-2 receptor α chain regulates the size and content of the peripheral lymphoid compartment, *Immunity 3* (4), 521−530.
5. Lodolce, J. P., et al. (1998) IL-15 receptor maintains lymphoid homeostasis by supporting lymphocyte homing and proliferation, *Immunity 9* (5), 669−676.
6. Nelson, B. H., and Willerford, D. M. (1998) Biology of the interleukin-2 receptor, *Adv. Immunol. 70*, 1−81.
7. Fehniger, T. A., and Caligiuri, M. A. (2001) Interleukin 15: Biology and relevance to human disease, *Blood 97* (1), 14−32.
8. Kobayashi, H., et al. (2000) Differences of biodistribution, pharmacokinetics, and tumor targeting between interleukins 2 and 15, *Cancer Res. 60* (13), 3577−3583.
9. Dubois, S., et al. (2002) IL-15Rα recycles and presents IL-15 in trans to neighboring cells, *Immunity 17* (5), 537−547.
10. Damjanovich, S., et al. (1997) Preassembly of interleukin 2 (IL-2) receptor subunits on resting Kit 225 K6 T cells and their modulation by IL-2, IL-7, and IL-15: A fluorescence resonance energy transfer study, *Proc. Natl. Acad. Sci. U.S.A. 94* (24), 13134−13139.
11. Lehours, P., et al. (2000) Subunit structure of the high and low affinity human interleukin-15 receptors, *Eur. Cytokine Network 11* (2), 207−215.
12. Bulanova, E., et al. (2001) The IL-15R α chain signals through association with Syk in human B cells, *J. Immunol. 167* (11), 6292−6302.
13. Dubois, S., et al. (200) Distinct pathways involving the FK506-binding proteins 12 and 12.6 underlie IL-2-versus IL-15-mediated proliferation of T cells, *Proc. Natl. Acad. Sci. U.S.A. 100* (24), 14169−14174.
14. Rao, B. M., et al. (2003) Interleukin-2 mutants with enhanced α-receptor subunit binding affinity, *Protein Eng. 16* (12), 1081−1087.
15. Stemmer, W. P. (1994) DNA shuffling by random fragmentation and reassembly: In vitro recombination for molecular evolution, *Proc. Natl. Acad. Sci. U.S.A. 91* (22), 10747−10751.
16. Boder, E. T., and Wittrup, K. D. (2000) Yeast surface display for directed evolution of protein expression, affinity, and stability, *Methods Enzymol. 328*, 430−444.
17. Rao, B. M., et al. (2004) *Mol. Pharmacol.* (in press).
18. Hori, T., et al. (1987) Establishment of an interleukin 2-dependent human T cell line from a patient with T cell chronic lymphocytic leukemia who is not infected with human T cell leukemia/lymphoma virus, *Blood 70* (4), 1069−1072.
19. Arima, N., et al. (1992) Pseudo-high affinity interleukin 2 (IL-2) receptor lacks the third component that is essential for functional IL-2 binding and signaling, *J. Exp. Med. 176* (5), 1265−1272.
20. Lakowicz, J. R. (1999) in *Principles of Fluorescence Spectroscopy*, pp 122−124, Kluwer Academic/Plenum Publishers, New York.
21. Fallon, E. M., et al. (2000) Increased endosomal sorting of ligand to recycling enhances potency of an interleukin-2 analog, *J. Biol. Chem. 275* (10), 6790−6797.
22. Smith, K. A. (1989) The interleukin 2 receptor, *Annu. Rev. Cell Biol. 5*, 397−425.
23. Zandstra, P. W., Lauffenburger, D. A., and Eaves, C. J. (2000) A ligand−receptor signaling threshold model of stem cell differentiation control: A biologically conserved mechanism applicable to hematopoiesis, *Blood 96* (4), 1215−1222.
24. Khaled, A. R., and Durum, S. K. (2002) Lymphocide: Cytokines and the control of lymphoid homeostasis, *Nat. Rev. Immunol. 2* (11), 817−830.
25. Marrack, P., and Kappler, J. (2004) Control of T cell viability, *Annu. Rev. Immunol. 22*, 765−787.
26. Guthridge, M. A., et al. (1998) Mechanism of activation of the GM-CSF, IL-3, and IL-5 family of receptors, *Stem Cells 16* (5), 301−313.
27. Fyfe, G., et al. (1995) Results of treatment of 255 patients with metastatic renal cell carcinoma who received high-dose recombinant interleukin-2 therapy, *J. Clin. Oncol. 13* (3), 688−696.
28. Atkins, M. B., et al. (1999) High-dose recombinant interleukin 2 therapy for patients with metastatic melanoma: Analysis of 270 patients treated between 1985 and 1993, *J. Clin. Oncol. 17* (7), 2105−2116.

BI050436X